High resolution optothermal spectroscopy of pyridine in the S-1 state

Becucci, M.; Lakin, N. M.; Pietraperzia, G.; Salvi, P. R.; Castellucci, E.; Kerstel, E. R. T.

Published in:
Journal of Chemical Physics

DOI:
10.1063/1.474203

High resolution optothermal spectroscopy of pyridine in the S_1 state

M. Becucci, N. M. Lakin, G. Pietraperzia, P. R. Salvi, E. Castellucci, and E. R. Th. Kerstel

Citation: J. Chem. Phys. **107**, 10399 (1997); doi: 10.1063/1.474203
View online: https://doi.org/10.1063/1.474203
View Table of Contents: http://aip.scitation.org/toc/jcp/107/24
Published by the American Institute of Physics

High resolution optothermal spectroscopy of pyridine in the S_1 state

M. Becucci,[a] N. M. Lakin, G. Pietraperzia,[b] P. R. Salvi,[b] and E. Castellucci[b]
European Laboratory for Non-Linear Spectroscopy (LENS), Largo E. Fermi 2, 50125 Firenze, Italy

E. R. Th. Kerstel
Department of Physics, University of Groningen, The Netherlands

(Received 14 July 1997; accepted 16 September 1997)

The optothermal technique has been utilized to obtain the first high resolution spectrum of pyridine in the region of the $S_1 \leftarrow S_0$ electronic transition. Rotational profiles for several vibronic bands (0_0^0,$6a_0^1$,$16b_0^2 6a_0^1$,$6a_0^2$,12_0^1) were measured and found to be severely homogeneously broadened with linewidths of the order of 3–5 GHz, in agreement with previous lifetime measurements. Rotational constants of pyridine in the excited S_1 vibronic levels were extracted by a band contour analysis. The values obtained are in good agreement with results from *ab initio* calculations, also presented here. © *1997 American Institute of Physics.* [S0021-9606(97)00248-1]

I. INTRODUCTION

The azabenzenes are considered prototypical systems of ''intermediate'' behavior in radiationless energy transfer.[1] Among these molecules, pyridine shows perhaps the least understood behavior in its first singlet state, S_1 ($^1B_1, n\pi^*$). In fact, pyridine is a difficult system to study under high resolution conditions using laser induced fluorescence (LIF) detection. While the $S_1 \leftarrow S_0$ oscillator strength (0.003) (Refs. 2, 3) is of the same order of magnitude as that of pyrazine and *s*-tetrazine,[4] the fluorescence quantum yield Φ_F is much lower (6×10^{-5}) (Ref. 5) in comparison with those of the other two molecules (0.02 and 0.001, respectively).[4]

It is generally believed that the low Φ_F value of pyridine is related to the $S_1 \rightarrow S_0$ internal conversion (IC) being more effective than $S_1 \rightarrow T_1$ intersystem crossing (ISC), the latter being the dominant process in most other azabenzenes (such as pyrazine[1] and pyrimidine[6,7]). This is supported by fluorescence lifetime measurements of pyridine vapor in a low pressure static cell, which are independent of the addition of SF_6 up to 100 Torr and show a strong dependence on the vibronic excitation.[5] Furthermore, the relaxation dynamics of S_1 pyridine has been studied in a pulsed laser, supersonic jet experiment by monitoring, as a function of the excess energy with respect to the S_1 zero point level (ZPL), both LIF and the formation of the triplet state.[8] Quantum yields of fluorescence and ISC of single vibronic levels were thereby determined. It was found that both Φ_F and Φ_{ISC} decrease rapidly with vibrational excitation $\geqslant 1600\ cm^{-1}$ above ZPL and that they become independent of the character of the excited vibronic band. This threshold coincides with the onset of the broad and congested band structure in the absorption spectrum. It was proposed[8] that the dominant decay process is IC induced by rapid intramolecular energy redistribution (IVR) in the statistical or ''large'' molecule limit. It was also suggested[8] that only an out-of-plane bending vibration could posses sufficient level density at the excitation energies involved. In subsequent studies with slightly higher spectral resolution (using the same pulsed laser, but with intracavity étalon) it was reported that the fluorescence quantum yield does not vary across the rotational envelope of the (0-0) $S_1 \leftarrow S_0$ band.[9,10]

In this paper we report high resolution measurements of several $S_1 \leftarrow S_0$ vibronic transitions of pyridine in a continuous supersonic molecular beam, using optothermal (OT) detection. Recently we demonstrated the advantages of this technique measuring OT spectra of weakly fluorescent systems, such as *s*-tetrazine and dimethyl-*s*-tetrazine, with a signal to noise ratio much larger than obtained by LIF detection under similar excitation conditions.[11] Up to now high resolution UV spectroscopy has relied almost exclusively on LIF detection. We report here the first example of a molecule for which the UV spectrum is measured at high resolution using OT detection prior to its observation at the same resolution by means of LIF. The study has enabled us to evaluate the rotational constants of the S_1 state, which were used to access the accuracy of a MO *ab initio* calculation of the equilibrium geometry. Furthermore, contour fits to the observed spectra, starting from a rigid rotor Hamiltonian, provide insight into the dynamics of the molecule in the S_1 state.

The experimental work is described in Sec. II. This is followed by data analysis and fitting (Sec. III A). The results of MO *ab initio* calculations are then presented (Sec. III B). The discussion (Sec. IV) is focused upon a comparison of rotational constants obtained from the calculated equilibrium geometries with the experimentally determined values. Finally the main points of the work are summarized (Sec. V).

II. EXPERIMENT

Pyridine (99% purity) was purchased from Aldrich and used without further purification.

The experimental apparatus has already been described in great detail in a previous report.[12] Briefly, the molecular beam machine consists of a source and a detection chamber. Pyridine is seeded in a flow of helium, which supersonically expands through a 50 μm nozzle into an evacuated chamber. The molecular beam, collimated by a conical skimmer, enters the detection chamber, where it interacts with the laser

[a]Author to whom correspondence should be addressed.
[b]LENS and Department of Chemistry, University of Florence, Italy.

beam. The molecular excitation may be detected by measuring either LIF or the energy content of the molecular beam by means of a bolometer cooled to 1.6 K. Nevertheless, in the present study we were able to observe only the high resolution OT spectrum of pyridine. A significant advantage of the OT detection system, compared to LIF, is the opportunity to greatly enhance the signal by multi-passing the laser through the molecular beam using a pair of plane, parallel reflectors. For the purpose of the present study, the broadband aluminum reflectors, used in previous experiments, were replaced by two dielectric mirrors with a peak reflectivity of 99.6% in the spectral range 280–290 nm. In addition, the distance between the mirrors was reduced from 70 to 25 mm. Using the new configuration, the optothermal signal due to the 0_0^0 ($S_1 \leftarrow S_0$) band absorption of aniline near 284 nm, was increased by a factor of about 20 compared with single crossing. The Doppler broadening of the signal, about 50 MHz, is however almost three times that obtained with the old arrangement.

The radiation source is a cw, single mode, ring dye laser (Coherent model 699-21) with KDP intracavity doubler, operating with Rhodamine-6G or Rhodamine 110 dyes. The laser has a linewidth of about 2 MHz and a power available at the crossing with the molecular beam in the range 0.5–2 mW. The molecular excitation is observed by amplitude modulation of the laser beam and phase sensitive detection of the bolometric signal by a lock-in amplifier. Relative and absolute frequency calibration are obtained from a reference étalon and a wavemeter, respectively. All the instrumentation is interfaced to a computer, which also controls the single mode scanning of the dye laser.

The observed rotational band contours were analyzed using a Fortran program, written specifically for the purpose and based on the ASYROT asymmetric rotor code.[13] The ground state rotational constants were held fixed at the values determined by microwave spectoscopy[14] and a Boltzmann distribution of the rotational populations was assumed. A simulated spectrum was obtained by convolution of the predicted rovibronic transitions with Lorentzians of a given width. The calculation was repeated over a grid of values for the rotational constants and linewidth. Each combination of constants was then assessed by least-squares fitting the simulation to the experimental spectrum with the intensity scale and band center as the only parameters. Data were given a weight of $1.0/n^2$ in the fit, where n is the estimated noise level. The standard deviation, σ, takes the unity value for a perfect fit. For each band only the combinations of constants giving contour fits with $\sigma \leqslant 1.5$ times the standard deviation of the best fit were retained. The constants were averaged over this set, each value being given a weight of $1.0/\sigma^2$. The standard deviation of the final contour fits for all five bands using the average constants were in the range 1.1–1.8. This type of analysis is facilitated by the simplicity of interpreting the intensity information obtained in a molecular beam experiment. While in gas cell experiments the rotational profiles are usually obscured by overlapping hot band structure, spectral congestion is considerably reduced in a molecular beam due to the efficient translational, rotational and vibrational cooling.

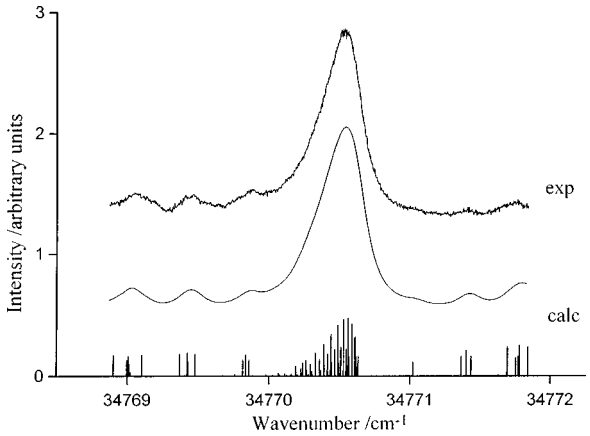

FIG. 1. Optothermal spectrum (expanded view) of pyridine in a continuous supersonic expansion (upper) in the region of the $S_1 \leftarrow S_0$ 0_0^0 vibronic transition and simulated spectrum (lower). The stick spectrum of rovibronic eigenstates and intensities is also shown under the simulated spectrum.

III. RESULTS

A. High resolution spectra

The OT signals due to bands 0_0^0, $6a_0^1$, $16b_0^2 6a_0^1$, $6a_0^2$ and 12_0^1 of the pyridine $S_1 \leftarrow S_0$ system have been measured in this work. The spectra of the 0_0^0 and $16b_0^2 6a_0^1$ bands, which are representative of all others, are shown in Figs. 1 and 2, respectively. These are characteristic of c-type (or perpendicular) transitions in an asymmetric near-oblate top. Each of them has a strong, unresolved Q branch surrounded by P and R branches consisting of several ''clumps'' of rotational transitions. The shading of the Q branch is mostly determined by the excited state C' rotational constant. The separation between adjacent clumps in the P and R branches depends on the parameter $(A'+B')/2$, while the dispersion of the transitions inside each clump depends on the asymmetry parameter $(A'-B')/2$; A' B' and C' being rotational

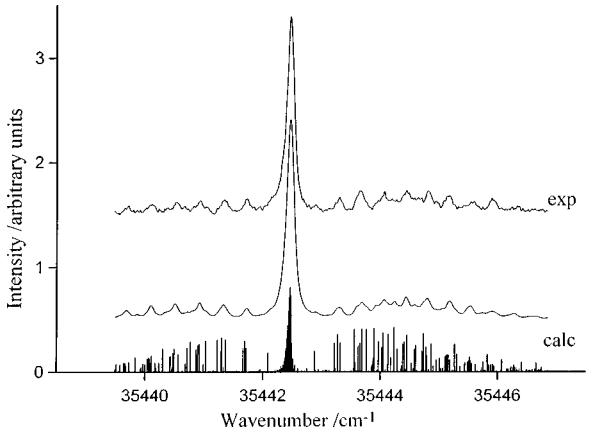

FIG. 2. Optothermal spectrum of pyridine in a continuous supersonic expansion (upper) in the region of the $S_1 \leftarrow S_0$ $16b_0^2 6a_0^1$ vibronic transition and simulated spectrum (lower). The stick spectrum of rovibronic eigenstates and intensities is also shown under the simulated spectrum.

TABLE I. Rotational parameters [$(A'+B')/2$, $(A'-B')/2$, C'; cm^{-1}], band origins (ν_0; cm^{-1}), inertial defect (Δ'; amu $Å^2$) and linewidths [Γ, full width at half maximum (FWHM); cm^{-1}] of the S_1 rovibronic levels 0^0, $6a^1$, $16b^26a^1$, $6a^2$ and 12^1 of pyridine obtained by band contour analysis.[a,b]

	0^0	$6a^1$	$16b^26a^1$	$6a^2$	12^1
ν_0	34770.54	35313.98	35442.48	35857.50	35767.64
$(A'+B')/2$	0.1927(34)	0.1936(28)	0.1965(19)	0.1934(24)	0.1910(20)
$(A'-B')/2$	0.0100(45)	0.0139(37)	0.0149(35)	0.0146(37)	0.0166(33)
C'	0.0955(8)	0.0967(14)	0.0980(8)	0.0984(14)	0.0992(11)
Δ'	0.9(41)	−0.9(45)	−0.5(27)	−4.1(40)	−7.9(29)
Γ[c]	0.186(24) 0.126(12)	0.141(26) 0.156(18)	0.106(15) 0.156(18)	0.146(23) 0.140(15)	0.176(11) 0.152(17)

[a]Ground state rotational constants constrained to the microwave values (Ref. 14).
[b]Values in round parentheses are one standard deviation of the parameter over the set of acceptable solutions ($\sigma \leqslant 1.5$; see text for details) in units of the last quoted decimal place.
[c]Upper values: this work; lower values: linewidths calculated from lifetime measurements and estimated error (Ref. 31).

constants in the S_1 state. Lifetime broadening (of the order of several GHz, far beyond the separation between adjacent single rovibronic lines) makes it impossible to resolve all individual transitions. The only P and R clumps with single eigenstate assigments are ${}^qR(0)$ and ${}^qP(1)$, observed with poor signal to noise ratio and obscured by the shading of the Q branch. Due to this the Lorentzian width of the transitions is varied in the simulations to achieve the best fit to experiment.

Previous work on pyridine and similar molecules suggests that the $S_1 \leftarrow S_0$ transition should be subject to a/b axis-switching.[9] Contour fits for all five vibronic bands were performed with and without the inclusion of axis-switching. In all cases, there was a small improvement in the standard deviation assuming the occurrence of axis-switching although the rotational constants were not appreciably different. This effect was clearly shown in the $16b_0^26a_0^1$ band, where the standard deviation of the contour fit improved by 13% with the inclusion of axis-switching. In addition, axis-switching is supported by our *ab initio* calculations. The results given in our tables therefore include axis-switching.

The rotational temperature best describing the experimental contours is approximately 6 K. A negligible improvement in the contour fits occurs by enlarging the basis set of rotational eigenfunctions to include those with quantum number $J \geqslant 16$. For each band the constants averaged over the acceptable solutions are given in Table I. Simulations of bands 0_0^0 and $16b_0^26a_0^1$ calculated with these values are shown in Figs. 1 and 2.

The parameter $(A'+B')/2$, dependent on the clump separation, and C', dependent on the shading of the Q branch, are determined more accurately than $(A'-B')/2$, which is related to the total dispersion within the P and R clumps. Consequently, determination of the inertial defect, Δ', can be quite inaccurate. In the case of the 0_0^0 band, which is subject to the largest error, the inertial defect varies over a wide range within the set of acceptable solutions (-10 to 11 amu $Å^2$) and its average value can be taken as zero within one standard deviation. The rotational constants, A', B' and especially C', given in Table I for the 0^0 S_1 level differ significantly from those of a past report.[9] Improved frequency resolution and a better suppression of hot band signals with our instrumentation results in a higher accuracy in the determination of these constants.

The rotational linewidths depend upon the vibronic band considered, varying in the range 3–5 GHz (see Table I). Our values are generally in good agreement with those resulting from previous lifetime measurements,[5,8] with the exception of the 0_0^0 band that shows a much larger linewidth.

B. Theoretical calculations

The ground and lowest excited states of pyridine have been studied by *ab initio* MO methods in a number of papers.[15–20] Reports of the equilibrium geometries and vibrational frequencies in the lowest singlet states S_n ($n \geqslant 1$) are however scarce.[16] In this work calculations for the first two excited states were performed using the 6-31G and DZV basis sets and including polarization orbitals (6-31G** and DZV** respectively). The multi-configurational self-consistent-field (MCSCF) wavefunction was obtained in the complete-active-space (CAS) of excited configurations, i.e., considering all possible promotions within a given set of molecular orbitals, which in our case are amongst the four highest valence ($3\pi+1n$) and three lowest virtual π^*. The corresponding wavefunction, MCSCF/CAS(4,3), is a linear combination of 490 configurations. Geometries and vibrational frequencies were then evaluated by applying the optimization procedures[21] and normal mode calculation[22,23] of the GAMESS package.[24]

Calculations for the ground state are in good agreement with the existing experimental data and are of a quality comparable with that of past reports.[15–17,20] In Table II, the calculated equilibrium geometry of S_0 is compared with the structure determined by microwave spectroscopy.[14] As it may be seen, starting from the relatively good 6-31G geometry the effect of including the polarization orbitals is to shorten the C-N bond and to increase the C-H bond lengths. Both of these changes are in the desired direction for a better agreement with the experimentally determined structure. A similar trend is found in going from the DZV to the DZV** basis set. Furthermore, the MCSCF/CAS(4,3) geometry cal-

TABLE II. Calculated geometries of the S_0, S_1 and S_2 states of pyridine with the 6-31G and the 6-31G** basis sets: pairs and triplets refer to bond lengths (Å) and angles (degrees) as indicated in the upper figure. Results from MCSCF/CAS(4,3) calculations (see text for details): experimental S_0 geometry from Ref. 4.

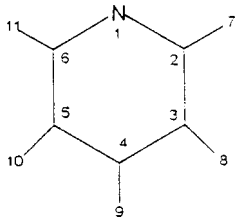

	S_0			S_1	S_2
	6-31G	6-31G**	exp	6-31G**	6-31G**
1-2	1.3453	1.3326	1.3376	1.3756	1.3698
2-3	1.3963	1.3948	1.3938	1.3634	1.4329
3-4	1.3972	1.3930	1.3916	1.4391	1.4336
2-7	1.0704	1.0760	1.0857	1.0701	1.0734
3-8	1.0720	1.0748	1.0818	1.0744	1.0733
4-9	1.0725	1.0754	1.0811	1.0719	1.0717
2-1-6	118.65	117.60	116.94	128.37	116.00
1-2-3	122.5	123.48	123.80	115.90	124.26
2-3-4	118.85	118.58	118.53	120.41	119.55
3-4-5	118.65	118.25	118.40	119.00	116.37
1-2-7	116.15	116.10	116.03	118.11	115.68
2-3-8	120.10	120.10	120.12	118.94	119.22
3-4-9	120.68	120.90	120.80	120.50	121.81

culated with the 6-31G** set is essentially the same as that obtained by extending the calculation to consider up to 8412 excited configurations.[15] In the latter the leading terms of the wavefunction expansion (apart from the closed-shell Hartree-Fock) are the same singly and doubly-excited $\pi\pi^*$ configurations which are obtained in the reduced calculation. The coefficients of these terms are also similar. This demonstrates that the promotion to virtual molecular orbitals higher than $3\pi^*$ has a minor effect on S_0.

The ground vibrational frequencies calculated using the 6-31G** basis set and the MCSCF/CAS(4,3) wavefunction are compared with previous experimental data in Table III. As is usual in *ab initio* calculations of vibrational frequencies, a systematic deviation is found between the calculated and experimental data. Empirical scaling of the former gives factors which are larger than 0.9 for all vibrations, except for $\omega_{16a}(a_2)$ (0.87). The averaged factor is 0.93. Although density functional theory would undoubtedly perform better for the ground state,[20] the above results are considered satisfactory for the present study.

We investigated the S_1 and S_2 states using a similar approach and in the following we shall refer only to calculations with the 6-31G** set, which gave the best results for the ground state. Excited state results are collected in Table II. Vibrational frequencies calculated for equilibrium C_{2v} geometries are all real for both states (see Table III). This indicates that these geometries correspond to minima on the potential energy surfaces of S_1 and S_2.

Given the potential minima and correcting for zero-point energies with the help of the calculated vibrational frequencies, the (0-0) transition energies may be obtained as shown in Table III. Whilst ΔE_0^0 (S_2-S_0) is almost coincident with the experimental band origin, ΔE_0^0 (S_1-S_0) is larger than the experimental value by $\approx 6\%$. The first result is consistent with the covalent nature of the first excited $\pi\pi^*$ state in aromatic molecules. In benzene, for example, previous SCF/CAS calculations have indicated that the $S_1(B_{2u})$ state is described mostly by $\pi\pi^*$ promotions and that the excitation energy is well reproduced also in less extended calculations. In accordance with this, the value of ΔE_0^0 (S_2-S_0) calculated for pyridine is weakly affected by basis change or by CI enlargement. Conversely, ΔE_0^0 (S_1-S_0) increases, up to reversal of energy ordering with respect to ΔE_0^0 (S_2-S_0), by including polarization orbitals or enlarging the CI calculation. This suggests that the S_1 state is not completely covalent and that a partially ionic character should be attributed. This might also explain the difference between calculated and experimental excitation energies in the 6-31G** calculation.

IV. DISCUSSION

The rotational constants of pyridine in the S_0, S_1 and S_2 states have been calculated from the equilibrium geometries optimized by means of the MCSCF/CAS(4,3) wavefunction and compared in Table IV with available experimental values. Table V reports the same comparison for the substituted molecule, pyridine-4-d_1, for which the rotational constants have been calculated assuming equilibrium geometries unchanged from the parent molecule.

TABLE III. Absolute energies (E(a.u.)), excitation energies ΔE (cm^{-1}) corrected by zero-point energies and normal frequencies (cm^{-1}) of pyridine in the S_0, S_1 and S_2 states (MCSCF/CAS(4,3) results; 6-31G** basis set).[a,b]

		S_0		S_1[c]	S_2[d]
		Obs	Calc	Calc	Calc
E(a.u.)			−246.782783	−246.609129	−246.603424
ΔE (cm^{-1})				36817	38406
ω (cm^{-1})					
a_1	2	3094	3373	3425	3402
	13	3073	3351	3394	3384
	20*a*	3030	3334	3365	3372
	8*a*	1584	1741	1693	1879
	19*a*	1483	1635	1537	1552
	9*a*	1218	1318	1256	1278
	18*a*	1072	1157	1099	1092
	12	1032	1107	988	984
	1	991	1059	964	978
	6*a*	601	646	594	565
b_2	20*b*	3087	3371	3419	3385
	7*b*	3042	3347	3366	3371
	8*b*	1581	1723	1633	1673
	19*b*	1442	1576	1471	1647
	14	1362	1492	1420	1490
	3	1227	1288	1321	1456
	15	1143	1155	1144	1234
	18*b*	1079	1135	907	982
	6*b*	652	706	649	642
b_1	5	1007	1032	899	732
	10*b*	941	982	688	647
	11	747	785	545	519
	4	703	734	527	485
	16*b*	406	450	80	290
a_2	17*a*	966	1023	902	772
	10*a*	871	912	562	664
	16*a*	373	429	428	299

[a]Experimental transition energies: $(0\text{-}0)(S_1 \leftarrow S_0)$, 34770 cm^{-1} (this work); $(0\text{-}0)(S_2 \leftarrow S_0)$, 38350 cm^{-1} (from Ref. 4).

[b]The normal vibrations in the ground state are classified according to Lord (Ref. 32).

[c]Observed S_1 frequencies and assignment from Ref. 4: 997 cm^{-1} (12, a_1), 542 cm^{-1} (6*a*, a_1), 484 cm^{-1} (11, b_1), 59 cm^{-1} (16*b*, b_1), 326 cm^{-1} (16*a*, a_2).

[d]Observed S_2 frequencies and assignment from Ref. 4: 950 cm^{-1} (1, a_1), 550 cm^{-1} (6*a*, a_1), 1215 cm^{-1} (unassigned), 327 cm^{-1} (unassigned).

There is excellent agreement between experiment and calculation for both S_0 and S_1 states of pyridine. Ground state calculated values differ from those determined by microwave spectroscopy[14] by only 0.04%–0.18%, while in the S_1 state the difference is 0.11%–1.65% (less than one standard deviation for A' and B' and only slightly larger for C'). The MO *ab initio* calculations confirm the occurrence of a/b axis-switching, determined experimentally. This results from the large structural change around the nitrogen atom in the S_1 state; both the C(6)N(1)C(2) angle and the N(1)-C(2) distance increase with respect to those in S_0. As a result, the labels of the in-plane principal axes, given in Table IV, are interchanged. The calculated equilibrium geometries of S_1 and S_2 are also consistent with the $n\pi^*$ and $\pi\pi^*$ character of these states. The $n \rightarrow \pi^*$ promotion, which contributes mostly to S_1, changes the geometry around the nitrogen atom. In contrast, the S_2 structure expands uniformly without appreciable variation of the bond angles from that for S_0.

An identical level of agreement between calculated and experimental rotational constants[25] is found for pyridine-4-d_1 in the S_0 state. For the S_1 state, however, the difference is considerably increased for A' (twice as large) and B' (more than one order of magnitude larger) compared to the unsubstituted molecule. Furthermore, these differences are greater than the reported experimental uncertainties.[26] Our *ab initio* calculations predict the occurrence of a/b axis-switching also for pyridine-4-d_1. The discrepancy probably results because axis-switching was not included in the model used for the band contour analysis and/or due to problems related to hot band structure. The gas phase spectra were taken in a static cell[26] and therefore should be particulary sensitive to the effects of axis switching, due to the population of highly excited rotational levels.

Over the past decade there has been much speculation about the geometry of pyridine in its S_1 state. The large reduction in frequency of the out-of-plane ''boat'' vibration, $\omega''_{16b}(b_1)$, in going from the S_0 (406 cm^{-1}) to the S_1 state (60 cm^{-1}) has been taken as evidence for the quasi-planarity of the excited state.[27] Fitting the vibrational intervals for this mode in the S_1 state to a simple potential function gave a double minumum with a small ($\approx$4 cm^{-1}) barrier height. In this case, however, a non-planar C_s geometry for S_1 would be expected to have an energy lower than that of the C_{2v} structure. This is not confirmed by our calculations. Nevertheless, a large decrease for $\omega_{16b}(b_1)$ in going from the ground to excited state (450 cm^{-1} to 80 cm^{-1}) is still calculated using the 6-31G** basis set. This change is not, however, sufficiently large to distort the S_1 energy surface. Changing the basis set to DZV**, the values for the same mode are 447 cm^{-1} in S_0 and 77 cm^{-1} in S_1. It seems unlikely that further improvements in the quality of the calculation will produce considerably different results. Previous 6-31G*/CIS calculations gave one imaginary b_1 frequency but these probably suffered from an insufficient CI expansion.[16] Our own calculations indicate that the pyridine equilibrium structure in S_1 is planar. The softening of the potential surface along the coordinate for the out-of-plane ''boat'' vibration implies the coupling of S_1 with upper A_1 states, most probably $S_4(A_1)$,[28] which is excited from the ground state in a strongly allowed transition at about 50 000 cm^{-1}.

The effective planarity of pyridine in the lowest vibrational level of S_1 is also supported by the value of zero (to within one standard deviation) obtained for the inertial defect, Δ (see Table I). Zero or slightly negative values for Δ are found for the other vibronic levels studied here. It has been proposed that the efficiency of the $S_1 - T_1$ ISC arises from vibronic perturbation of S_1 by higher lying $\pi\pi^*$ states.[8] According to our results, the effect is not sufficient to produce a non-planar equilibrium geometry for S_1. The value of the inertial defect for the 12^1 level is surprisingly

TABLE IV. Rotational constants A, B, C (cm^{-1}) of pyridine from band contour analysis and calculated A, B, C values (MCSCF/CAS(4,3) wavefunction, 6-31G** basis set) corresponding to the minima of S_0, S_1 and S_2 states.[a,b]

	S_0		S_1		S_2
	Expt[c,d]	Calc[d]	Expt[c,d]	Calc[d]	Calc[d]
A	0.201447(75) $[z]$	0.2018 $[z]$	0.2027(67) $[y]$	0.2062 $[y]$	0.1956 $[z]$
B	0.193631(01) $[y]$	0.1935 $[y]$	0.1827(43) $[z]$	0.1828 $[z]$	0.1823 $[y]$
C	0.0987086(77) $[x]$	0.0988 $[x]$	0.0955(8) $[x]$	0.0969 $[x]$	0.0944 $[x]$

[a]Values in round parentheses are one standard deviation of the parameter over the set of acceptable solutions ($\sigma \leqslant 1.5$; see text for details) in units of the last quoted decimal place.

[b]The coordinate axis parallel to the principal axis of interest is indicated in square parentheses. The z-axis lies along the C(4)-N(1) direction, the y-axis is the second in-plane axis and the x-axis is perpendicular to the molecular plane.

[c]Ground state rotational constants are from microwave spectroscopy (Ref. 14); S_1 rotational constants from this work.

[d]Experimental values refer to the $v=0$ level; calculated values to the equilibrium structures of S_0, S_1 and S_2 (see Table III).

large and negative since excitation of an in-plane vibration is expected to produce only a small positive contribution to Δ.

Finally, it should be noted that our S_1 rotational profiles support the view of coupling of this state with S_0 rather than T_1.[8] The efficiency of the relaxation process is controlled, among other factors, by the available density of states.[29] The total vibronic S_0 density at the vibrationless level of S_1 ($\Delta E \approx 34\,770\ cm^{-1}$) may be estimated (in the harmonic approximation and using the Laplace transform method of Romanini and Lehmann[30]) to be $\approx 10^{13}/cm^{-1}$ while that of T_1 at the same energy (with the singlet-triplet energy gap $\Delta E \approx 5130\ cm^{-1}$ (Ref. 4) and the vibrational frequencies assumed equal to those of S_0 for the sake of simplicity) $\approx 220/cm^{-1}$. Considering only the combination states due to totally-symmetric fundamentals as available for efficient coupling[29] the two densities are lowered to $\approx 10^4/cm^{-1}$ and $1/cm^{-1}$, respectively. At our experimental resolution (≈ 50 MHz) the vibronic states of S_0 near S_1 effectively form a continuum, whereas the triplet manifold may be considered a sparse distribution of levels. Coupling between S_1 and T_1 in such a case should give rise to resolvable spectral irregularities and/or line splittings. Although the individual rotational lines are not resolved, there is no clear evidence of such effects in our observed spectra. In fact, the smooth contours observed in our spectra strongly suggest that coupling to S_0 must occur, in agreement with previous lifetime measurements. Experiments at even higher sensitivity and resolution, including double resonance to selectively excite single rovibronic eigenstates, may be envisaged to test this conclusion.

TABLE V. Rotational constants A, B, C (cm^{-1}) of pyridine-4-d_1 from band contour analysis and calculated A, B, C values (MCSCF/CAS(4,3) wavefunction, 6-31G** basis set) corresponding to the minima of S_0, S_1 and S_2 states.[a,b]

	S_0		S_1		S_2
	Expt[c,d]	Calc[d]	Expt[c,d]	Calc[d]	Calc[d]
A	0.20144 $[z]$	0.2018 $[z]$	0.19843(8) $[y]$	0.1920 $[y]$	0.1956 $[z]$
B	0.18079 $[y]$	0.1807 $[y]$	0.17957(8) $[z]$	0.1828 $[z]$	0.1704 $[y]$
C	0.09526 $[x]$	0.0953 $[x]$	0.09426(20) $[x]$	0.0936 $[x]$	0.0911 $[x]$

[a]Values in round parentheses are one standard deviation of the parameter in units of the last quoted decimal place.

[b]The coordinate axis parallel to the principal axis of interest is indicated in square parentheses. The z-axis lies along the C(4)-N(1) direction, the y-axis is the second in-plane axis and the x-axis is perpendicular to the molecular plane.

[c]Ground state rotational constants are from microwave spectroscopy (Ref. 25); S_1 rotational constants from Ref. 26.

[d]Experimental values refer to the $v=0$ level; calculated values to the equilibrium structures of S_0, S_1 and S_2 (see Table III).

V. CONCLUSIONS

In this paper we report the first high resolution spectrum of the $S_1 \leftarrow S_0$ transition of pyridine in a supersonic expansion. The traditional difficulties in observing this transition because of the low fluorescence quantum yield of pyrdine in its S_1 state were overcome by the use of optothermal detection. Accurate estimates of upper state rotational constants have been extracted from the band contours. Comparison with the results from *ab initio* calculations, suggests a planar equilibrium geometry for S_1 pyridine. Rotational line profiles, in as far as they may be determined, support IC as the dominant S_1 decay channel.

ACKNOWLEDGMENTS

This work was supported by the E.C. under the Contracts CHRX-CT-0561, ERBFMBICT961046, ERBCHRXCT930105, and ERBFMGECT950017.

[1] J. Kommandeur, W. A. Majewski, W. L. Meerts, and D. W. Pratt, Annu. Rev. Phys. Chem. **38**, 433 (1987).
[2] S. F. Mason, J. Chem. Soc. Part I, 1240 (1959).
[3] L. Goodman, J. Mol. Spectrosc. **6**, 100 (1961).
[4] K. K. Innes, I. G. Ross, and W. R. Moomaw, J. Mol. Spectrosc. **132**, 492 (1988).
[5] I. Yamazaki, K. Sushida, and H. Baba, J. Chem. Phys. **71**, 381 (1979).
[6] W. L. Meerts and W. A. Majewski, Laser Chem. **5**, 339 (1986).
[7] J. A. Konings, W. A. Majewski, Y. Matsumoto, D. W. Pratt, and W. L. Meerts, J. Chem. Phys. **89**, 1813 (1988).
[8] E. Villa, A. Amirav, and E. C. Lim, J. Phys. Chem. **92**, 5393 (1988).

[9] A. Meenakshi, W. Chen, and E. C. Lim, Chem. Phys. Lett. **148**, 507 (1988).
[10] Y. D. Shin and E. C. Lim, Chem. Phys. Lett. **151**, 308 (1988).
[11] E. R. Th. Kerstel, M. Becucci, G. Pietraperzia, and E. Castellucci, J. Chem. Phys. **106**, 1318 (1997).
[12] E. R. Th. Kerstel, M. Becucci, G. Pietraperzia, and E. Castellucci, Chem. Phys. **199**, 263 (1995).
[13] T. J. Sears, Comput. Phys. Commun. **34**, 123 (1984).
[14] F. Mata, M. J. Quintana, and G. O. Sorensen, J. Mol. Struct. **42**, 1 (1977).
[15] I. C. Walker, M. H. Palmer, and A. Hopkirk, Chem. Phys. **141**, 363 (1989).
[16] J. B. Foresman, M. Heat-Gordon, J. A. Pople, and M. J. Frisch, J. Phys. Chem. **96**, 135 (1992).
[17] M. P. Fulscher, K. Andersson, and B. D. Roos, J. Phys. Chem. **96**, 9204 (1992).
[18] K. B. Wiberg, J. Mol. Struct. **244**, 61 (1990).
[19] W. H. Yang and G. C. Schatz, J. Chem. Phys. **97**, 3831 (1992).
[20] J. M. L. Martin and C. Van Alsenoy, J. Phys. Chem. **100**, 6973 (1996).
[21] J. Baker, J. Comput. Chem. **7**, 385 (1986).
[22] W. D. Gwinn, J. Chem. Phys. **55**, 477 (1971).
[23] P. Pulay, G. Fogarasi, and J. E. Boggs, J. Am. Chem. Soc. **101**, 2550 (1979).
[24] M. Dupuis, D. Spangler, and J. J. Wendoloski, NRCC Software Catalog, Vol. 1, program No. QG01, GAMESS, University of California, 1980.
[25] B. Bak, L. Hansen, and J. Rastrup-Andersen, J. Chem. Phys. **22**, 2013 (1954).
[26] F. W. Birss, S. D. Colson, and D. A. Ramsay, Can. J. Phys. **51**, 1031 (1973).
[27] J. P. Jesson, H. W. Kroto, and D. A. Ramsay, J. Chem. Phys. **56**, 6257 (1972).
[28] P. J. Chappel and I. G. Ross, Chem. Phys. Lett. **43**, 440 (1976).
[29] B. R. Henry and W. Siebrand, in *Organic Molecular Photophysics* (Wiley, New York, 1973), Vol. 1.
[30] D. Romanini and K. K. Lehmann, J. Chem. Phys. **98**, 6437 (1993).
[31] I. Yamazaki, T. Murao, K. Yoshihara, M. Fujita, K. Sushida, and H. Baba, Chem. Phys. Lett. **92**, 421 (1982).
[32] R. C. Lord, A. L. Marston, and F. A. Miller, Spectrochim. Acta **9**, 113 (1957).